Structural retrofit of Eastern Canada's existing masonry using geosynthetics: preliminary test results

M. El-Assaly [1 [0009-0009-3606-5221]]; G. Aubry[1]; S. Bhat[2] ; M.A. Meguid [1 [0000-0002-5559-194X]] and D. Malomo [1 [0000-0002-4518-5841]]

[1] McGill University, Montreal, QC, H3A 0C3, Canada
[2] CTO Geosynthetics, Titan Environmental Containment Ltd., MB, R0A 0T1, Canada

Abstract. Canada's building stock consisting of unreinforced masonry (URM) components is facing a consistent threat. Nearly 50% of URM structures were built before 1970 which makes them vulnerable to seismic events, settlements and floods that are furthermore intensified with climate change. Retrofitting old URM structures is a key solution to enhance life safety, avoid possible demolition and deconstruction that are contributing to Canada's increasing solid wastes. Unlike traditional retrofitting techniques, using polymeric materials for retrofitting is becoming a versatile approach due to it being cost-effective, durable and a non-invasive option. This paper aims to use polypropylene geogrid material as a strengthening option for old URM buildings. The experimental campaign consists of six double wythes wallets that are constructed using solid clay bricks, type O mortar with addition of sand to replicate the structural properties of old URM buildings. Two specimens are considered control specimens and the remaining four underwent retrofitting with geogrid overlays as a seismic system intervention for in-plane loads. Each sample was loaded in compression diagonally, causing a diagonal tension failure following the ASTM E519 guidelines. Design parameters of the adopted strengthening system included different configurations. Results exhibited improved in-plane shear strength and displacement capacity.

Keywords: Structural retrofit, textile reinforced mortar, geosynthetics, in-plane, diagonal compression test, unreinforced masonry

1 Introduction

In this study, textile reinforced mortar (TRM) using geosynthetics are introduced as a non-invasive, low-cost, and fast installation repair/retrofitting technique for unreinforced masonry (URM). In Eastern Canada, the majority of its building stock are pre-1970 URM, which makes them particularly vulnerable to natural hazards, e.g, earthquakes, settlements, etc. [1]. The lack of maintenance and aging coupled with the impacts of climate change are reducing the already sub-stranded structural and energy performance of the above-mentioned URM buildings.

Nationally, structural retrofit research has mostly focused on traditional means of reinforcing such as, steel [2], concrete [3], and fiber-reinforced materials [4]. With the national Building Code of Canada (NBCC) requiring existing building to meet modern standards in an event of renovations, and despite the increasing interest in converting existing buildings into housing, the challenge of avoiding environmentally impactful demolitions is still open. This area of research remains largely unexplored in North America. In this context, the novelty of the following study stems from exploring geosynthetics as a retrofit alternative tailored for the Canadian market – with an overarching goal of facilitating affordable building reuse, with a less-invasive renovation approach targeting life safety (LS) structural performance, as per ASCE 41-23 [5].

Geosynthetics materials are primarily used to enhance and stabilize earth structures that are subject to different surface loading conditions [6]. For reinforcing earth structures (e.g., geogrids), they are typically installed at relatively shallow depth, as a result, the mechanical stresses and thermal effects are affected due to temperature variations [7]. Geogrids are manufactured using various materials, including ductile poly-polymeric (PP) composites and high-stiffness fiberglass (FG). Both these above-mentioned materials have the unexplored potential to provide increased load-capacity and ductility the URM lacks. The use of geogrids have progressively increased due to their ability to enhance both the in-plane and out-of-plane behaviour of masonry panels [8]–[15]. They are mostly adopted to strengthen structural components, improve performance of arches and vaults or to confine columns or pillars [11], [16]–[18]. In addition to all these applications, the use of geogrids offers enhanced tensile strength, feasibility, versatility, and corrosion resistance [11]. While URM walls have adequate capacity for vertical loading, their ability to resist lateral loads are considered not sufficient by current standards. Retrofitting with a low-stiffness material such as geogrids can offer an increase in the resistance of lateral loads and control the mode of failure during a seismic event. Giaretton et al. [12] conducted diagonal compression testing on 11 two-leaf thick solid clay brick wallets with dimensions of 1030 mm × 1030 mm × 120 mm (L × H × T). Three wallets remained unreinforced, while five were strengthened using a single-sided configuration and three using a double-sided configuration. The strengthening material consisted of a multi-axial hybrid glass-polypropylene composite. The results demonstrated that retrofitted wallets exhibited superior performance compared to the unreinforced specimens. The shear capacity increased by factors of 1.5 and 2.6 for the single-sided and double-sided strengthening configurations, respectively. Similarly, Banerjee et al. [15] conducted a comparable study, extending their investigation to both clay and fly-ash bricks. A total of 32 wallets were casted and retrofitted using two different techniques. In the first approach, wallets were wrapped with polypropylene bands and secured using clips and fasteners. While in the second approach, a wire mesh was attached to the masonry surface and overlaid with a strengthening mortar (1:3, cement: sand). The polypropylene-based retrofitting technique resulted in significant improvements in load-carrying capacity and shear strength. Overall, both retrofitting methods enhanced the shear strength of clay brick and fly-ash brick wallets by over 80% and 100%, respectively.

The objective of the ongoing study held at McGill Struct-lab investigates the use of ductile PP geogrid as an effective solution for retrofitting brittle URM structures and components. The solution proposed in this paper offers preliminary results on diagonal compression testing (DCT) performed on geogrid retrofitted wallets. The results are analyzed to compare the bond behaviour, strength, and failure mode.

2 Experimental characterization of ductile geogrids

Geosynthetics have temperature dependent properties and are prone to exhibit a wide range of behaviour depending on the exposure, temperature and environmental conditions [19]–[21]. Therefore, it is critical to assess the mechanical behaviour and properties of geogrids over a range of temperature through a detailed testing campaign to simulate what they may be exposed to during their service life. R. Desbrousses et al. [22] performed a series of uniaxial tensile tests on PP geogrids that are primarily used for railroad constructions under the influence of different temperature. The testing included two different aperture sizes of the same PP geogrid. The property of each material is reported in Table 1, as well as, Figure 1 (a) and (b) which shows both the small aperture size of the geogrid (35x35 mm) and the bigger size (57x57 mm) respectively. It is noted that the main focus in this study is the small aperture size, henceforth we refer to it whenever using "PP geogrid".

Table 1. Properties of PP geogrid

Property	Large biaxial geogrid	Small biaxial geogrid
Material	PP	PP
Ultimate tensile strength	30/30 kN/m	30/30 kN/m
Aperture size	57/57 mm	38/38 mm
Rib thickness	1.8/1.2 mm	2.3/1.5 mm

The single-rib tensile test was performed in accordance with method A, ASTM D6637 [23]. As per ASTM D6637, test specimens are comprised of single ribs and require an increase in the load on specimens until failure. Figure 1 (c) shows a single yarn for the PP geogrid. The tensile test was performed using an MTS testing system equipped with a temperature chamber so that specimens remain in a temperature-controlled environment throughout the test. The temperature chamber is equipped with a Thermcraft medium range heater/cooler system for reaching and maintaining the targeted temperatures. Figure 1 shows a schematic diagram for the testing machine used on PP geogrids.

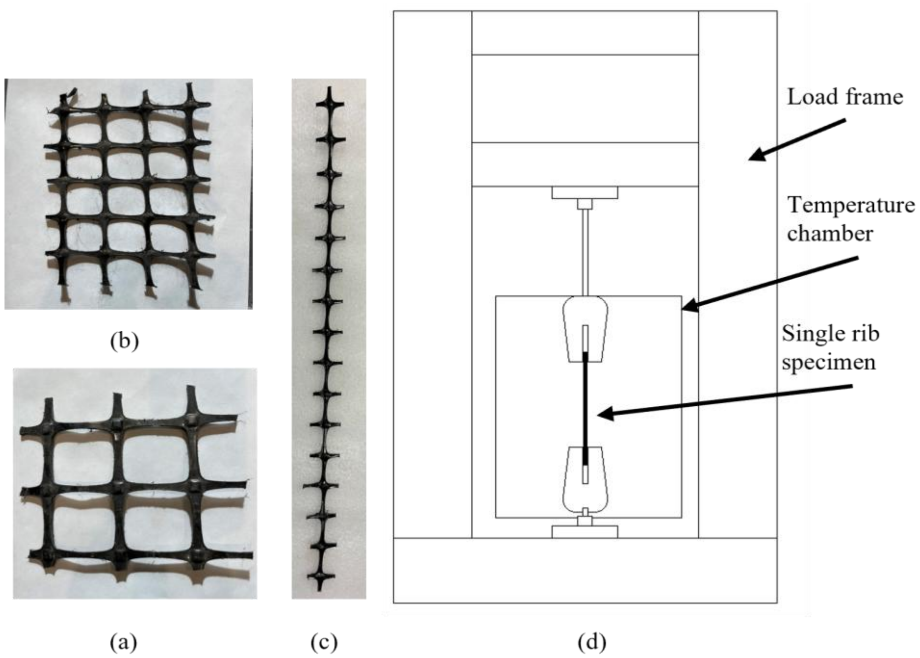

Figure 1. (a) Large size PP geogrid, (b) small size PP geogrid, (c) single rib specimen, and (d) schematic test-setup used to perform tensile test

PP geogrids were found to be temperature sensitive. Lower tensile strength accompanied by high strain values were recorded as the temperature surged and vice versa. Tensile strength decreased by 15% at 40 C whereas at -30 C, tensile strength increased by 34%. At 20°C, the PP geogrid exhibited failure characterized by the junction splitting in half. As the temperature increased to 30°C and 40°C, the geogrid's junctions display extreme distortion; however, no significant failure was observed at the rib cross-section. Conversely, at lower temperatures, as the PP geogrid lost its ability to elongate, the failure mode shifted to sudden fracture, accompanied by fibers protruding from the sides of the ribs.

3 Experimental characterization of masonry constituents

Structural testing was conducted at McGill University's Jamieson Structural Laboratory. Six double-wythe URM walls (0.6x0.6x0.2 m3) were constructed based on data from actual walls extracted from an existing building in Montreal [24]. Walls were constructed by professional masons and left curing for at least 28 days in a humidity-controlled environment with monitored RH between 30%-70% as per ASTM-S304 [25], see Figure 2 (a). Two walls were left without retrofitting (URM1, URM2) and two walls were fitted with full configuration PP geogrid mortar overlay (RP-URM1, PR-URM2). Following the ASTM-E519 [26] standards while introducing minor alteration in terms of specimen size, diagonal compression testing was performed through rotating the wallets at a 45 ˚ angle to simulate earthquake and settlement effects through diagonal compressive load centered at wall corners, see Figure 2 (b). Displacement controlled loading rate was applied and maintained as 0.3 mm/min, while data were recorded and monitored using linear variable differential transformers (LVDTs), as well as digital image correlation (DIC) to supplement the traditional LVDTs placed along both the compression and tension struts. A metal frame was created specifically for handling, transporting, and rotating the wallets as shown in Figure 2 (c). Two loading steel shoe and wooden panels were used to ensure uniform load distribution. RP-URM1 and RP-URM2 were strengthened in a single side configuration, with the PP geogrid sandwiched between a 20mm layer of type O mortar. Additionally, four anchors were used to hold and mechanically engage with the geogrid, see Figure 3(a). The anchors (ϕ1.27 mm and 203 mm length) were welded to a hexagon steel plate to ensure the connection of the mesh to the bricks. The strengthening application encompassed the following steps: (i) Application of first later of type O mortar (thickness 10 mm), (ii) placement and positioning of the PP geogrid, (iii) fixation of the PP geogrid with anchors, (iv) applying the second layer of type O mortar (thickness 10 mm), see Figure 3 (b, c).

Figure 2 (a) Walls casting, (b) DCT setup, and (c) lifting/rotational device

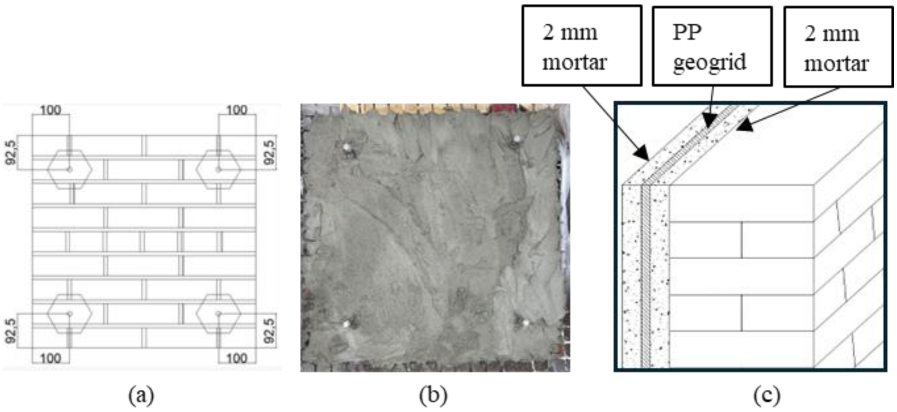

Figure 3 (a) Anchor distribution, (b) Applied PP geogrid and mortar overlay, and (c) schematic overview of retrofitting system

The URM wallets were casted with the purpose to replicate old masonry mechanical properties that are typically found in Eastern Canada. Glen-gery solid clay bricks and altered type O mortar with 15% added sand to match existing URM's compressive strength were also tested along side the wall as a part of the testing campaign. Following the CSA-A179 [27] and CSA-A82 [28], the compressive strength for the mortar cubes was 1.71 MPa (COV=3.91%) and that of bricks 43.4 MPa (COV=19%). Furthermore, following the ASTM-C1072 standards [29], bond wrench testing was conducted on 5 doublets to evaluate the flexural bond between the masonry substrates; the flexural bond F_g was 0.46 MPa (COV=17%).

4 Experimental results

All URM wallets experienced diagonal shear failure (i.e., URM1, URM2, RP-URM1, and RP-URM2), therefore, according to EQ. $\tau = P\cos\alpha / 0.5t(H+L)$ (1) reported by the ASTM E519, the diagonal force was converted into shear stress.

$$\tau = P\cos\alpha / 0.5t(H+L) \quad (1)$$

τ is the shear stress, P is the applied maximum diagonal force, α is the angle between the diagonal and horizontal axis of the wall, t, H, and L are the thickness, height, and length of the wall, respectively. The shear strain was calculated according to Eq. $\gamma = \Delta C + \Delta T / g$ (2)

$$\gamma = \Delta C + \Delta T / g \quad (2)$$

where γ is the shear strain, ΔC, ΔT are the diagonal compression side and the diagonal tensioning side, respectively, and g is the gauge length. Since all the wallets exhibited diagonal shear failure, the secant shear modulus, G, was determined between 5% and 70 % of τ_{max} from the shear stress-strain curves according to [30]. The shear strength and shear modulus for the 4 wallets and available literature are reported in Table 2 below. It is noteworthy that the un-retrofitted wallets examined in this study exhibited significantly higher peak values compared to similar specimens reported in the literature, this is stemming from using different mortar types and different clay bricks that has different compressive strength.

(a) (b)

Figure 4 (a) Crack pattern for URM1, (b) crack pattern for RP-URM1

Additionally, available literature indicates that single-sided strengthening approach may result in a lower maximum diagonal load compared to un-retrofitted wallets. This reduction is attributed to the asymmetric reinforcement, which induces stiffness irregularities [12], [31]. The latter statement corresponds to the values reported in Table 2. Both RP-URM1 and RP-URM2 exhibited higher shear modulus values compared to URM1 and URM2, with recorded values of 2.75, 2.62, 2.09, and 2.10, respectively.

Table 2 Shear strength and modulus for as built and retrofitted wallets

Specimen	**Retrofit**	**Peak load (kN)**	τ_{max} **(MPa)**	***G*** **(GPa)**	**Failure mode**
URM 1	N/A	202	1.25	2.09	DF
URM 2	N/A	145	0.90	2.10	DF
RP-URM 1	PP mesh	181	1.12	2.75	DF/SF
RP-URM 2	PP mesh	155	0.96	2.62	DF/SF
Giaretton et al.[12]	N/A	99.2	0.26	1.92	DF
Giaretton et al. [12]	Multiaxial hybrid glass PP	148.0	0.39	2.61	DF
Banerjee et al. [15]	N/A	32.5	0.71	0.81	DF
Banerjee et al. [15]	PP bands with clips	70.5	0.84	0.99	DF

Note: DF: diagonal failure; SF: sliding failure; τ_{max}: Peak shear stress

URM 1 and 2 exhibited a diagonal failure (DF) behaviour in both mortar joint and bricks at the corners of the wall, see Figure 4(a). Unlike RP-URM 1 and 2 who demonstrated a combination of both diagonal failure and sliding failure (SF). Figure 4 (b) shows the formation of multiple cracks on the strengthened surface, this mainly occurred due to the uniform distribution of stresses caused by the PP geogrid mesh across the face of the wallet. Small displacement was expected and showed due to the brittle failure, reaching 0.466 and 0.336 mm for both URM 1 and URM 2. On the other hand, RP-URM 1 and RP-URM 2 showed much higher maximum compressive displacement reaching 35 times on average and up to 49 times (URM2 vs RP-URM1), with 16.46 mm for RP-URM 1 and 11.74 mm for RP-URM 2. The force displacement response of the replicated specimens is shown in Figure 5 and Figure 6. URM 1 and URM 2 curves exhibit a positive slope until the propagation of diagonal cracks followed by a sudden brittle failure, both reached a peak load of 202 kN and 145 kN respectively. Moreover, Table 3 shows that RP-URM1 and 2 reached peak values of 181 kN and 155 kN, respectively. The ratio between load at maximum displacement against peak load (f_u/f_{max}) was 55 and 40 for RP-URM 1 and RP-URM 2 respectively. Additionally, the ratio between the displacement at peak load and the maximum displacement reached 1.5 and 2.4 for RP-URM 1 and RP-URM 2, respectively. The curves in Figure 6 for retrofitted walls show that after peak load, a drop of 79 kN and 94 kN for RP-URM1 and 2, respectively. The retrofitted wallets recovered an average of 48 % of loadbearing capacity following the initiation of the first diagonal crack.

Table 3 DCT results (C is compression strut and T stands for tension tie)

Wall	**Peak load (kN)**	**τ_{max} (MPa)**	**Max displ. – C (mm)**	**Max. displ. – T (mm)**	**f_u/f_{max} (%)**	**d_u/d_{max} (%)**
URM 1	202	1.25	0.466	0.325	N/A	N/A
URM 2	145	0.90	0.336	0.307	N/A	N/A
RP-URM 1	181	1.12	16.44	16.46	55	1.5
RP-URM 2	155	0.96	11.74	14.62	40	2.4

Note: τ_{max}: max shear stress; f_u: load at max. displ.; f_{max}: peak load; d_u: displ. at peak load; d_{max}: max. displ.

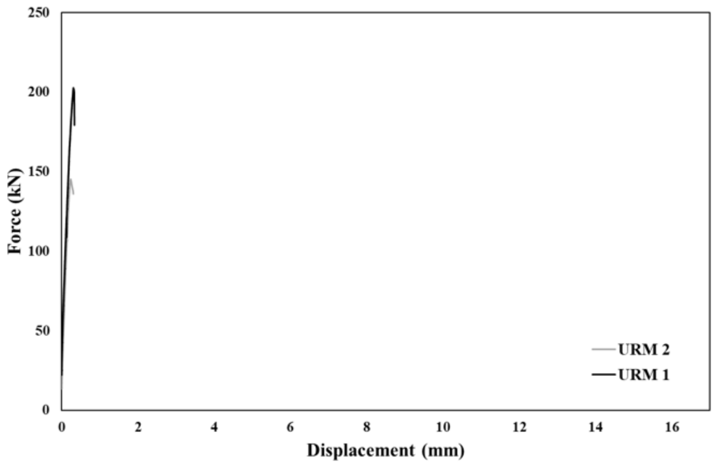

Figure 5 Force vs. displacement for URM 1 and 2

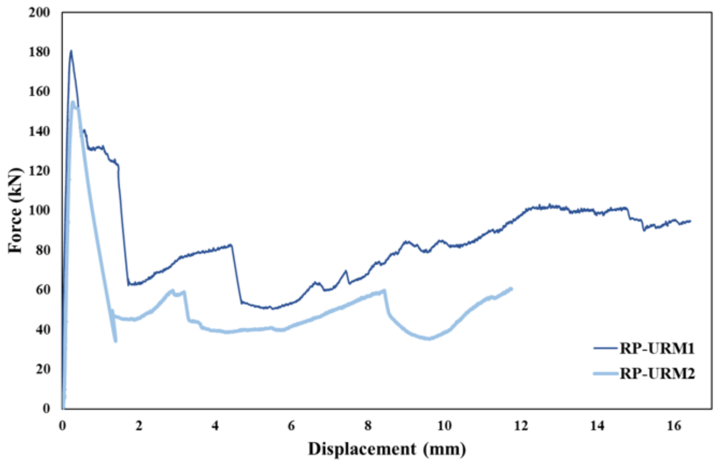

Figure 6 Force vs. displacement for RP-URM1 and 2

5 Conclusions

In this study, the mechanical performances of a novel geosynthetics-based retrofitting system using polypropylene (PP) geogrids are evaluated experimentally. The scope of the proposed design is to improve the in-plane (IP) behaviour of existing unreinforced masonry (URM) buildings typical of Eastern Canada, by enhancing the displacement capacity and avoiding brittle failures, hence contributing to achieve life safety thresholds set by ASCE 41-23[5]. A total of four URM wallets were casted and tested to capture the failure modes, crack patterns, maximum loads, and shear stress through diagonal compression testing according to ASTM-E519 (albeit used smaller URM samples). Diagonal compression testing (DCT) performed at McGill University's Jamieson structural laboratory highlights the effectiveness of the retrofit by increasing the displacement capacity, while also inducing more ductile failure mechanisms. The four wallets were casted by professional masons using weakened type O mortar to replicated old URM buildings. The following conclusions can be drawn from the observed experimental results, which are this stage must be intended as preliminary:

- The proposed retrofitting approach enhanced the displacement capacity and overall structural performance of the URM wallets by 40 % (RP-URM1), and 30 % (RP-URM2).

- The application of PP geogrid retrofit altered the failure mode from a brittle diagonal failure to a ductile shear-compression sliding mechanism.

- The observed failures occurred through the mortar joints and bricks, no debonding of the strengthening layer or rupture of the PP geogrid was observed.

- Retrofitted wallets retained a relevant percentage of their initial (undamaged) loadbearing capacity after initial cracking: 55 % (RP-URM1), and 40 % (RP-URM2).
- PP geogrid showed significant improvement in failure strains and was able to delay the brittle failure often experienced with un-strengthened URM.

The following study solely focuses on quantifying the structural performance of PP geogrid retrofit through conducting in-plane monotonic diagonal compression testing on 0.6 m x 0.6 m URM wallets. Further investigations are required to assess the structural performance under both quasi-static cyclic and dynamic loading, as well as under out-of-plane actions. The proposed PP geogrid retrofit system offers a promising and an under-explored solution for enhancing the resilience of existing URM buildings in Eastern Canada. Ongoing research and testing aim to optimize the retrofitting system through enlarging the specimen size, exploring different configurations, and different materials such as fiberglass. These findings offer significant contributions to the field of sustainable building retrofitting and present strong potential for practical implementation across Eastern Canada.

Acknowledgement

The authors acknowledge funding received by NSERC, Mitacs and Titan Environmental Containment Inc. through the NSERC-Mitacs Alliance program. The authors thank Dr. Desbrousses for his contribution in characterizing the PP geogrid, a testing campaign that was useful for experimental testing.

References

[1] American Institute of Architects, "The Business of Architecture: 2020 AIA Firm Survey Report," New York City, USA, 2020.

[2] P. Mottier, R. Tremblay, and C. Rogers, "Seismic retrofit of low-rise steel buildings in Canada using rocking steel braced frames," *Earthq. Eng. Struct. Dyn.*, vol. 47, no. 2, pp. 333–355, Feb. 2018, doi: 10.1002/EQE.2953.

[3] M. Zarrabi, R. Bartosh, and A. Pall, "Seismic Rehabilitation of Les Jardins Westmount, Montreal (Quebec), Canada," *15th World Conf. Earthq. Eng.*, 2012.

[4] A. A. Hamid, W. W. El-Dakhakhni, Z. H. R. Hakam, and M. Elgaaly, "Behaviour of Composite Unreinforced Masonry–Fiber-Reinforced Polymer Wall Assemblages Under In-Plane Loading," *J. Compos. Constr.*, vol. 9, no. 1, pp. 73–83, 2005, doi: 10.1061/(asce)1090-0268(2005)9:1(73).

[5] R. Pekelnicky and C. Poland, "ASCE 41-13: Seismic Evaluation and Retrofit Rehabilitation of Existing Buildings," *SEAOC 2012 Conv. Proc.*, 2012.

[6] M. Shokr, M. A. Meguid, and S. Bhat, "Experimental Investigation of the Tensile Response of Stiff Fiberglass Geogrid Under Varying Temperatures," *Int. J. Geosynth. Gr. Eng.*, vol. 8, no. 1, pp. 1–8, 2022, doi: 10.1007/s40891-022-00361-7.

[7] M. Li and Y. G. Hsuan, "Temperature and pressure effects on the degradation of polypropylene tape yarns - Depletion of antioxidants," *Geotext. Geomembranes*, vol. 22, no. 6, pp. 511–530, 2004, doi: 10.1016/j.geotexmem.2004.06.001.

[8] F. Ferretti, M. Canestri, and C. Mazzotti, "Effect of temperature variations on the bond behaviour of FRCM applied to masonry," *Mater. Struct. Constr.*, vol. 55, no. 6, pp. 1–14, 2022, doi: 10.1617/s11527-022-02002-x.

[9] C. Faella, E. Martinelli, E. Nigro, and S. Paciello, "Shear capacity of masonry walls externally strengthened by a cement-based composite material: An experimental campaign," *Constr. Build. Mater.*, vol. 24, no. 1, pp. 84–93, 2010, doi: 10.1016/j.conbuildmat.2009.08.019.

[10] A. Bellini, A. Incerti, M. Bovo, and C. Mazzotti, "Effectiveness of FRCM Reinforcement Applied to Masonry Walls Subject to Axial Force and Out-Of-Plane Loads Evaluated by Experimental and Numerical Studies," *Int. J. Archit. Herit.*, vol. 12, no. 3, pp. 376–394, 2018, doi: 10.1080/15583058.2017.1323246.

[11] M. R. Valluzzi *et al.*, "Round Robin Test for composite-to-brick shear bond characterization," *Mater. Struct. Constr.*, vol. 45, no. 12, pp. 1761–1791, 2012, doi: 10.1617/s11527-012-9883-5.

[12] M. Giaretton, D. Dizhur, E. Garbin, J. M. Ingham, and F. da Porto, "In-Plane Strengthening of Clay Brick and Block Masonry Walls Using Textile-Reinforced Mortar," *J. Compos. Constr.*, vol. 22, no. 5, pp. 1–10, 2018, doi: 10.1061/(asce)cc.1943-5614.0000866.

[13] A. Dalalbashi, B. Ghiassi, and D. V. Oliveira, "A multi-level investigation on the mechanical response of TRM-strengthened masonry," *Mater. Struct. Constr.*, vol. 54, no. 6, 2021, [Online]. Available: https://doi.org/10.1617/s11527-021-01817-4

[14] S. Banerjee, S. Nayak, and S. Das, "Adjudging efficacy of geonet reinforcement on the seismic performance of brick masonry structures: an experimental study," *Mater. Struct. Constr.*, vol. 54, no. 6, pp. 1–24, 2021, doi: 10.1617/s11527-021-01805-8.

[15] S. Banerjee, S. Nayak, and S. Das, "Improving the In-Plane Behaviour of Brick Masonry Wallet Using PP Band and Steel Wire Mesh," *J. Mater. Civ. Eng.*, vol. 32, no. 6, pp. 1–15, 2020.

[16] L. Ascione, L. Feo, and F. Fraternali, "Load carrying capacity of 2D FRP/strengthened masonry structures," *Compos. Part B Eng.*, vol. 36, no. 8, pp. 619–626, 2005.

[17] D. Baraldi, E. Reccia, and A. Cecchi, "In plane loaded masonry walls: DEM and FEM/DEM models. A critical review," *Meccanica*, vol. 53, no. 7, pp. 1613–1628, May 2018, doi: 10.1007/s11012-017-0704-3.

[18] G. de Felice *et al.*, "Recommendation of RILEM Technical Committee 250-CSM: Test method for Textile Reinforced Mortar to substrate bond characterization," *Mater. Struct. Constr.*, vol. 51, no. 4, pp. 1–9, 2018, doi: 10.1617/s11527-018-1216-x.

[19] D. I. Bush, "Variation of long-term design strength of geosynthetics in temperatures up to 40 C," in *Proceedings of the Fourth International. Conference on Geotextiles, Geomembranes, and Related Products*, 1990, pp. 673–676.

[20] R. M. Koerner, Y. Hsuan, and A. E. Lord Jr, "Remaining technical barriers to obtaining general acceptance of geosynthetics," *Geotext. Geomembranes*, vol. 12, no. 1, pp. 1–52, 1993.

[21] J. Han and Y. Jiang, "Use of geosynthetics for performance enhancement of earth structures in cold regions," *Sci. Cold Arid Reg.*, vol. 5, no. 5, pp. 517–529, 2013.

[22] R. L. E. Desbrousses, M. A. Meguid, and S. Bhat, "Effect of Temperature on the Mechanical Properties of Two Polymeric Geogrid Materials," *Geosynth. Int.*, no. 0, 2021, doi: 10.1680/jgein.21.00032a.

[23] ASTM International, "Standard test method for determining tensile properties of geogrids by the single or multi-rib tensile method (ASTM-D6637:15)." 2015.

[24] L. Davis and D. Malomo, "Typological Evolution of Old Industrial Masonry Buildings in Eastern Canada for Holistic Seismic Assessment, Upgrading and Reuse," in *International Conference on Structural Analysis of Historical Constructions*, 2023, pp. 43–55.

[25] Canadian Standards Association, *CSA S304-14 Design of Masonry Structures*. 2014.

[26] ASTM, "Standard Test Method for Diagonal Tension (Shear) in Masonry Assemblages (ASTM-E519:02)," pp. 1–5, 2002, [Online]. Available: www.astm.org,

[27] CSA-A179-14, *National Standard of Canada CAN / CSA-A179-14 Mortar and grout for unit masonry*, vol. 14, no. JULY 2015. 2014.

[28] CSA, *National Standard of Canada Fired masonry brick made from clay or shale (CSA A-A82:18)*, no. March. 2018.

[29] ASTM, "Standard Test Method for Measurement of Masonry Flexural Bond Strength (ASTM-C1072)," pp. 681–692, 2006.

[30] D. Dizhur and J. M. Ingham, "Diagonal tension strength of vintage unreinforced clay brick masonry wall panels," *Constr. Build. Mater.*, vol. 43, pp. 418–427, 2013, doi: 10.1016/j.conbuildmat.2013.02.015.

[31] M. R. Valluzzi, D. Tinazzi, and C. Modena, "Shear behaviour of masonry panels strengthened by FRP laminates," *Constr. Build. Mater.*, vol. 16, no. 7, pp. 409–416, 2002, doi: 10.1016/S0950-0618(02)00043-0.